Hydrothermal Synthesis and Structure of [H₄As^III₂As^VMo^V₈Mo^VI₄O₄₀]⁻, A Bicapped, Reduced Keggin Species

M. Ishaque Khan, Qin Chen and Jon Zubieta*

Department of Chemistry, Syracuse University, Syracuse, New York 13244

Received November 17, 1992

The hydrothermal reaction of As_2O_3, MoO_3, NaCl, and water in a mole ratio of 5:10:10:380 for 50 h at 150 °C yielded a dark blue solution, which upon standing produced blue-black crystals of $Na_{0.5}H_{4.5}[As_3Mo_{12}O_{40}]\cdot 4H_2O$ (1). The structure of the anion of **1** $[H_4As_3Mo_{12}I_{40}]^-$ consists of an α-Keggin core $\{AsMo_{12}O_{40}\}$ capped on opposite $\{Mo_4O_4\}$ faces by As(III) groups. The anion is a mixed-valence species with eight Mo(V) and four MO(VI) centers. Crystal data for $As_3Mo_{12}Na_{0.5}O_{44}H_{12.5}$: Triclinic space group $P\bar{1}$, $a = 13.609(3)$ Å, $b = 14.177(3)$ Å, $c = 10.584(2)$ Å, $\alpha = 111.02(1)°$, $\beta = 98.95(2)°$, $\gamma = 90.15(1)°$, $V = 1879.2(9)$ Å³, $Z = 2$, $D_{calc} = 3.711$ g cm⁻³; structure solution and refinement were based on 7301 reflections converging at $R = 0.0518$.

Reduced polyoxoanions have received considerable attention in recent years as a consequence of their unusual electronic properties,[1–4] interesting structural chemistries,[5–7] and importance in catalysis.[8–10] For the heteropolyanion class of clusters, the W/As/O system has been extensively studied, and As(III) has been demonstrated to provide a template for the synthesis of a variety of unusual polyanions.[11–15] In contrast, the Mo/As/O system has remained relatively unexplored. The mixed-valence species $[H_4As^VMo^V_4Mo^{VI}_8O_{40}]^{3-}$ and $[H_2As^VMo^V_2Mo^{VI}_{10}O_{40}]^{3-}$[16] have been shown to possess Keggin-type structures, thus providing relatively rare examples of crystalline mixed-valence polyanions.

In the course of our investigations of the hydrothermal reactions of metal oxides, we have prepared an eight-electron reduced mixed valence Mo^V/Mo^{VI}, As^{III}/As^V cluster containing the α-Keggin core, $[H_4As^{III}_2As^VMo^V_8Mo^{VI}_4O_{40}]^-$ (**1a**). The results provide a further demonstration of the effectiveness of hydrothermal synthesis in the isolation of mixed valence polyanion clusters.[5,6]

Experimental Section

Reagent grade chemicals were used throughout. Arsenic(III) oxide, molybdenum(VI) oxide (Alfa), and sodium chloride (Aldrich) were used as received from the commercial sources. Electrochemical studies were performed on a BAS-100 electroanalytical system. Elemental analyses were performed by Oneida Research Laboratories, Oneida, NY.

(1) Pope, M. T. *Heteropoly and Isopoly Oxometalates*; Springer-Verlag: Berlin, 1983.
(2) Casañ-Pastor, N.; Gomez-Romero, P.; Jameson, G. B.; Baker, L. C. W. *J. Am. Chem. Soc.* **1991**, *113*, 5658 and references therein.
(3) Sanchez, C.; Livage, J.; Doppelt, P.; Chanveau, F.; Lefebre, J. *J. Chem. Soc., Dalton Trans.* **1982**, 2439.
(4) Darrows, J. N.; Jameson, G. B.; Pope, M. T. *J. Am. Chem. Soc.* **1985**, *107*, 1771.
(5) Khan, M. I.; Chen, Q.; Zubieta, J. *Inorg. Chem.* **1992**, *31*, 1556.
(6) Khan, M. I.; Chen, Q.; Goshorn, D. P.; Hope, H.; Parkin, S.; Zubieta, J. *J. Chem. Soc.* **1992**, *114*, 3341.
(7) Chen, Q.; Goshorn, D. P.; Scholes, C. P.; Tan, X.-L.; Zubieta, J. *J. Am. Chem. Soc.* **1992**, *114*, 4667.
(8) Haber, J. *The Role of Molybdenum in Catalysis*; Climax Molybdenum: London 1981.
(9) Mansuy, D.; Bartoli, J.-F.; Battioni, P.; Lyon, D. K.; Finke, R. G. *J. Am. Chem. Soc.* **1991**, *113*, 7222 and references therein.
(10) Renneke, R. F.; Pasquali, M.; Hill, C. L. *J. Am. Chem. Soc.* **1990**, *112*, 6885 and references therein.
(11) Martin-Frère, J.; Jeannin, Y.; Robert, F.; Vaisserman, J. *Inorg. Chem.* **1991**, *30*, 3635.
(12) Hervé, G. *Inorg. Synth.* **1990**, *27*, 118; Robert, F.; Leyrie, M.; Hervé, G.; Tezi, A.; Jeannin, Y. *Inorg. Chem.* **1990**, *19*, 1746.
(13) Leyrie, M.; Martin-Frère, J.; Hervé, G. *C. R. Acad. Sci., Ser. C.* **1974**, *279*, 895.
(14) Tourné, C.; Revel, A.; Tourné, G.; Vendrell, M. *C. R. Acad. Sci., Ser. C* **1973**, *277*, 643.
(15) Martin-Frère, J.; Jeannin, Y. *J. Am. Chem. Soc.* **1981**, *103*, 1664.
(16) Müller, A.; Krickemeyer, E.; Penk, M.; Wittenben, V.; Döring, J. *Angew. Chem., Int. Ed. Engl.* **1990**, *29*, 88.

Synthesis of $Na_{0.5}H_{4.5}[As_3Mo_{12}O_{40}]\cdot 4H_2O$. Arsenic(III) oxide, molybendum(VI) oxide, sodium chloride and water in the mole ratio 5:10:10:380 (0.99 g:1.44 g:0.595 g:6.84 g) were heated for 50 h at 150 °C in a 23-mL Teflon-lined acid digestion bomb. After being cooled to room temperature, the resulting dark blue solution was allowed to stand for 2–7 days, after which deep blue-black crystals of $Na_{0.5}H_{4.5}[As_3Mo_{12}O_{40}]\cdot 4H_2O$ were collected in low yield (5–10%). The crystals were collected by filtration, washed with cold water, and air dried. The crystals are soluble in water, acetone, acetonitrile, and methanol. IR(KBr pellet, cm⁻¹): 959 (vs), 942 (sh), 843 (vs). Anal. Calcd for $H_{12.5}Na_{0.5}O_{44}As_3Mo_{12}$: H, 0.59; Na, 0.55; As, 10.7. Found: H, 0.43; Na, 0.66; As, 10.8. Sodium was determined by atomic spectroscopy.

Crystal Structure Analysis. A summary of crystal parametes and experimental conditions is provided in Table I. A complete description of the crystallographic methods is given in the supplementary materials.

The structure was solved by direct methods and refined by full-matrix least-squares methods. Further details of the structure solution and refinement are presented in the supplementary material. The Na^+ cation is found to be partially disordered about the center of symmetry, resulting in a relatively large temperature factor. The crystal also contains disordered solvent molecules of crystallization of the following types and occupancies: O(41), 0.80; O(42), 0.70; O(43), 0.50; O(44), 0.50; O(45), 0.50; O(46), 1.00. The total water content is approximately 4.0 per asymmetric unit. Loss of approximately 2.5 water molecules occurs quite rapidly at room temperature and results in collapse of the crystallinity. In order to maintain crystal stability, crystals were mounted directly from the mother liquor and immediately immersed in the stream of the cold arm at –80 °C.

Electrochemical Studies. Cyclic voltammetric studies and controlled potential electrolyses were carried out in acetonitrile solution 1.0×10^{-3} M in complex and 0.1 M in $(n\text{-}C_4H_9)_4NPF_6$ as supporting electrolyte. Platinum-bead and platinum-mesh working electrodes were used in the cyclic voltammetry and controlled-potential electrolyses, respectively. All potentials are referenced to the ferrocene/ferrocenium couple.

Results and Discussion

Preparation and Characterization of $Na_{0.5}H_{4.5}[As_3Mo_{12}O_{40}]\cdot 4H_2O$. The reaction of arsenic(III) oxide, molybdenum(VI) oxide, NaCl, and water in the mole ratio 5:10:10:380 for 50 h at 150 °C and autogenous pressure yielded a deep blue solution. When this solution was allowed to stand for periods of 2–7 days, shiny blue-black crystals of a material analyzing for $Na_{0.5}H_{4.5}[As_3Mo_{12}O_{40}]\cdot 4H_2O$ (**1**) were isolated in low yield, generally *ca.* 5%. The infrared spectrum of **1** exhibited features characteristic of $\nu(Mo=O)$, $\nu(Mo—O—Mo)$ and $\nu(As—O)$ in the 840–960-cm⁻¹ region; weak bands at 3430 cm⁻¹ and 1600 cm⁻¹ indicated the presence of water.

Thermogravimetric analysis of a sample of **1** confirmed the presence of weakly associated H_2O and of considerable amounts of As in the composition. As shown in Figure 1, a weight loss

Table I. Crystallographic Data for 1

formula	$As_3Mo_{12}Na_{0.5}H_{12.5}O_4$
fw	2104.1
space group	$P\bar{1}$
a, Å	13.609(3)
b, Å	14.177(3)
c, Å	10.584(2)
α, deg	111.02(1)
β, deg	98.95(2)
γ, deg	90.15(1)
V, Å^3	1879.2(9)
D_{calc}, g cm^{-3}	3.711
μ(Mo Kα), cm^{-1}	66.2
radiation	Mo Kα, λ = 0.710 73 Å
T, °C	−80
transm factors: max; min	1.00; 0.516
R^a	0.0518
$R_w{}^b$	0.0550

^{a} $R = \sum\|F_o\| - \|F_c\|/\sum\|F_o\|$. ^{b} $R_w = [\sum(w(\|F_o\| - \|F_c\|)^{1/2}]/\sum(w\|F_o\|)^{1/2}$; w^{-1} = $[\sigma^2(\|F_o\|) + g\|F_o\|^2]$.
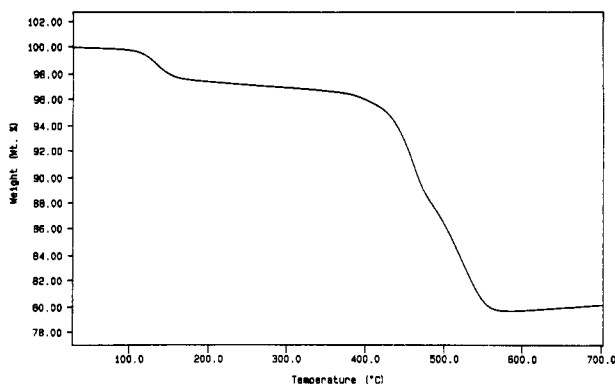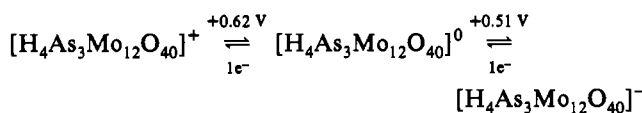

Figure 1. Thermogravimetric profile of **1** in the temperature range 25–700 °C.

of *ca.* 2% between 100 and 150 °C is associated with the loss of two water molecules. The water content of **1** as formulated is consistent with a weight loss 3.4%; however, samples of **1** used for thermogravimetric analyses had been removed from the mother liquor and dried for several hours prior to use. Subsequent studies revealed that crystals treated in this fashion lost between 1 and 2% weight while standing at room temperature, as a consequence of solvent loss. A further 17% weight loss occurs between 425 and 550 °C in two stages, corresponding to the loss of arsenic oxide as As_4O_6 vapor (16.4% theoretical loss).

Electrochemical Studies. The oxidation/reduction properties of **1** in acetonitrile were studied by cyclic voltammetry and controlled potential electrolysis. The cyclic voltammogram of **1** exhibited anodic as well as cathodic waves. Complex **1** showed two successive reversible one-electron oxidations at moderately positive potentials, 0.51 V and 0.62 V, with respect to ferrocene/ferrocenium, as shown in Figure 2a. The processes are judged electrochemically reversible on the basis of the ratio of peak heights for the anodic and cathodic waves (*ca.* 1.0) and the peak to peak separations (65 and 72 mV, respectively). Controlled-potential electrolysis of **1** at +0.70 V results in a color change from the characteristic blue to pale green after electrolysis with the consumption of 2 faraday mol^{-1}. Examination of the anolyte by CV after the two-electron oxidation showed that the single major product underwent successive one-electron reductions at +0.62 and +0.51 V to regenerate **1**.

$$[H_4As_3Mo_{12}O_{40}]^+ \underset{1e^-}{\overset{+0.62\ V}{\rightleftharpoons}} [H_4As_3Mo_{12}O_{40}]^0 \underset{1e^-}{\overset{+0.51\ V}{\rightleftharpoons}}$$
$$[H_4As_3Mo_{12}O_{40}]^-$$

Cyclic voltammetric sweeps to negative potentials reveal that **1** undergoes an irreversible multiple electron reduction at −1.37
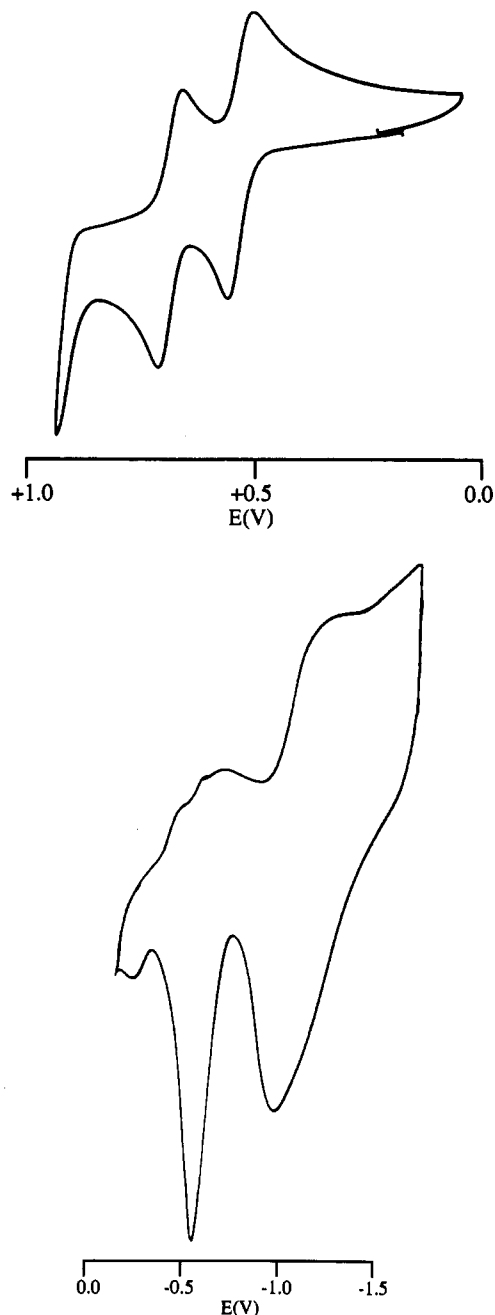

Figure 2. (a) Top: Cyclic voltammogram of a 1.0×10^{-3} M solution of **1** in 0.1 M (n-C$_4$H$_9$)$_4$NPF$_6$ acetonitrile. The potential measured at a Pt bead electrode at 200 mV s^{-1} is referenced to the ferrocene/ferrocenium couple. The potential range 0.0 to +1.0 V is shown. (b) Bottom: Cyclic voltammogram of **1** under the same conditions as those employed above, showing the 0.0 to −1.60 V range.

V. Controlled-potential electrolysis at −1.45 V indicates a four-electron process, suggesting that all 12 Mo centers of the cluster have been reduced to the MO(V) state. The reverse sweep of the cyclic voltammograms reveals an oxidation process related to the multi-electron cluster reduction and a second anodic process at −0.65 V (Figure 2b). The absence of a cathodic wave associated with this matter process demonstrates unambiguously an irreversible process, and a linear dependence of the current i_p on the sweep rate v indicates adsorption of some species on the electrode surface prior to oxidation (Figure 2b). Consistent with the theory of irreversible surface reactions,[17] the oxidation peak had a characteristic asymmetric shape, with a rapid decrease of i_p to a level approximately equal to that before the oxidation. The

(17) Laviron, E. *J. Electroanal. Chem. Interfacial Electrochem.* **1974**, *52*, 355.
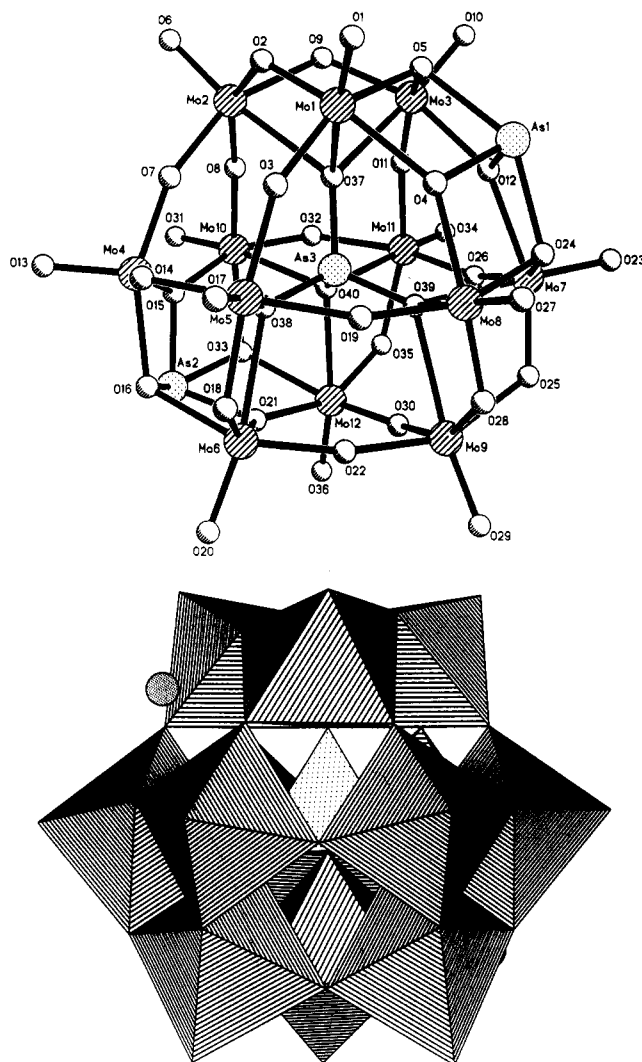
Figure 3. (a) Top: View of the structure of the molecular anion [H$_4$As$_3$Mo$_{12}$O$_{40}$]$^{1-}$ (**1a**) showing the atom-labeling scheme. (b) Bottom: Polyhedral representation of the structure of **1a**. The As(III) centers are shown as dotted spheres.

Table II. Atomic Coordinates ($\times 10^4$) and Equivalent Isotropic Displacement Coefficients (Å^2 $\times$ 10^3) for 1

	x	y	z	U(eq)^a
Mo(1)	8327(1)	5316(1)	−2471(1)	16(1)
Mo(2)	10100(1)	6921(1)	−48(1)	16(1)
Mo(3)	8924(1)	7746(1)	−2493(1)	15(1)
Mo(4)	8721(1)	6545(1)	2507(1)	16(1)
Mo(5)	6886(1)	5020(1)	77(1)	16(1)
Mo(6)	6187(1)	7095(1)	2470(1)	15(1)
Mo(7)	6079(1)	8375(1)	−2496(1)	15(1)
Mo(8)	5477(1)	5933(1)	−2493(1)	16(1)
Mo(9)	4865(1)	8066(1)	−93(1)	15(1)
Mo(10)	9397(1)	9280(1)	2491(1)	14(1)
Mo(11)	8128(1)	10043(1)	57(1)	14(1)
Mo(12)	6845(1)	9830(1)	2462(1)	15(1)
As(1)	6985(1)	6366(1)	−4252(1)	19(1)
As(2)	7990(1)	8674(1)	4243(1)	18(1)
As(3)	7496(1)	7516(1)	1(1)	11(1)
Na	0	5000	5000	78(4)
O(1)	8396(7)	4189(7)	−3739(9)	26(3)
O(2)	9611(6)	5610(6)	−1564(8)	20(3)
O(3)	7806(6)	4972(6)	−1182(8)	20(3)
O(4)	6875(6)	5680(6)	−3094(8)	17(3)
O(5)	8482(6)	6244(6)	−3544(8)	20(3)
O(6)	11307(7)	6762(8)	317(11)	29(4)
O(7)	9504(7)	6476(6)	1213(9)	21(3)
O(8)	9923(6)	8274(6)	1199(8)	18(3)
O(9)	10064(6)	7439(6)	−1563(9)	19(3)
O(10)	9336(7)	8021(7)	−3747(8)	23(3)
O(11)	8778(6)	8984(7)	−1195(9)	21(3)
O(12)	7380(6)	7661(6)	−3104(8)	18(3)
O(13)	9516(7)	6350(6)	3758(9)	21(3)
O(14)	8035(7)	5303(6)	1596(9)	21(3)
O(15)	8890(6)	8141(6)	3117(8)	19(3)
O(16)	7588(6)	7158(6)	3579(8)	19(3)
O(17)	6575(7)	3803(7)	−284(10)	28(3)
O(18)	6142(6)	5711(6)	1558(8)	19(3)
O(19)	5936(7)	5397(6)	−1181(9)	21(3)
O(20)	5510(7)	7213(7)	3700(9)	24(3)
O(21)	6835(6)	8570(6)	3058(8)	18(3)
O(22)	5343(6)	7388(6)	1162(9)	19(3)
O(23)	5731(8)	8835(7)	−3743(9)	27(3)
O(24)	5698(6)	6856(6)	−3563(8)	18(3)
O(25)	5008(6)	8556(6)	−1600(8)	17(3)
O(26)	6916(6)	9391(6)	−1200(9)	20(3)
O(27)	4765(7)	4980(7)	−3746(9)	23(3)
O(28)	4564(6)	6728(6)	−1605(8)	17(3)
O(29)	3749(6)	8400(7)	257(9)	24(3)
O(30)	5762(7)	9201(6)	1181(9)	21(3)
O(31)	10381(7)	9841(7)	3740(9)	25(3)
O(32)	9229(6)	10162(6)	1567(8)	19(3)
O(33)	8249(6)	9818(6)	3559(8)	18(3)
O(34)	8350(7)	11043(6)	−331(9)	23(3)
O(35)	7325(6)	10566(6)	1555(8)	17(3)
O(36)	6378(7)	10700(7)	3720(9)	23(3)
O(37)	8374(6)	7026(6)	−966(8)	17(3)
O(38)	7379(6)	6821(6)	965(8)	14(2)
O(39)	6390(6)	7468(6)	−967(8)	16(3)
O(40)	7847(6)	8740(6)	968(8)	16(3)
O(41)	7263(10)	2627(10)	3319(13)	48(3)
O(42)	6219(10)	3145(10)	5230(14)	53(3)
O(43)	7183(18)	2244(18)	7372(24)	41(5)
O(44)	8666(17)	1948(17)	5298(23)	37(5)
O(45)	5568(21)	873(21)	6301(29)	55(7)
O(46)	−1285(39)	4097(39)	3338(54)	124(16)

^{a} Equivalent isotropic U defined as one-third of the trace of the orthogonalized U$_{ij}$ tensor.

shape results from the negligible number of molecules that are brought to the electrode by diffusion during the potential sweep compared to the amount adsorbed. At midheight, the peak width is independent of the applied sweep rate and results in a value of 2.0 for αn_α. Since the symmetry factor α usually falls in the range of 0.5,[18] approximately four electrons are transferred in the rate-limiting step. This adsorption wave is only observed subsequent to the reductive process at −1.37 V; if the cathodic sweep is reversed before passing through this multielectron reductive process, no anodic wave is observed at −0.65 V. Controlled-potential electrolysis of **1** in acetonitrile at −1.45 V followed by cyclic voltammetry of the catholyte yields voltammograms qualitatively similar to those of H$_3$[AsMo$_{12}$O$_{40}$]·xH$_2$O[19] with the additional anodic peak at −0.65 V. This observation suggests that the multiple electron reduction of **1** at −1.37 V results in the release of As(III) from the cluster and its subsequent adsorption onto the electrode to produce the multielectron oxidation wave at −0.65 V.

Structure of 1. The crystal structure determination of **1** revealed the presence of discrete water molecules of crystallization, sodium cations, and the molecular anions [H$_4$As$_3$Mo$_{12}$O$_{40}$]$^-$ (**1a**), shown in Figure 3. In gross geometric terms, the structure of **1a** is best described as an α-Keggin core {Mo$_{12}$AsO$_{40}$} capped on two

oppositely disposed faces by As(III) to produce idealized D_{2d} point symmetry. The structure is reminiscent of that of [H$_4$PV$_{14}$O$_{42}$]$^{5-}$,[20,21] which consists of the {PV$_{12}$O$_{40}$} α-Keggin core capped by two {VO} units.

The structure of **1a** reveals the presence of both As(III) and As(V) sites. The central {As(V)O$_4$} tetrahedron shares its oxygen

(18) Bockris, J., O'M; Gochev, A. *J. Phys. Chem.* **1986**, *90*, 5232.
(19) Contant, R. *C. R. Acad. Sci. Paris* **1968**, *267*, 1479.

(20) Kato, R.; Kobayaski, A.; Sasaki, Y. *Inorg. Chem.* **1982**, *21*, 240.
(21) Khan, M. I.; Zubieta, J.; Toscano, P. *Inorg. Chim. Acta* **1992**, *193*, 17.

Table III. Selected Bond Lengths (Å) for 1

Mo(1)-O(1)	1.692(8)	Mo(1)-O(2)	1.827(8)
Mo(1)-O(3)	1.838(10)	Mo(1)-O(4)	2.109(8)
Mo(1)-O(5)	2.051(10)	Mo(1)-O(37)	2.371(7)
Mo(1)-NaA	3.686(1)	Mo(2)-O(2)	1.998(7)
Mo(2)-O(6)	1.664(9)	Mo(2)-O(7)	1.943(10)
Mo(2)-O(8)	1.940(7)	Mo(2)-O(9)	1.983(10)
Mo(2)-O(37)	2.424(8)	Mo(3)-O(5)	2.055(8)
Mo(3)-O(9)	1.843(9)	Mo(3)-O(10)	1.682(11)
Mo(3)-O(11)	1.835(8)	Mo(3)-O(12)	2.091(8)
Mo(3)-O(37)	2..402(10)	Mo(4)-O(7)	1.839(10)
Mo(4)-O(13)	1.679(9)	Mo(4)-O(14)	1.843(8)
Mo(4)-O(15)	2.118(9)	Mo(4)-O(16)	2.064(9)
Mo(4)-O(38)	2.384(8)	Mo(5)-O(3)	1.951(10)
Mo(5)-O(14)	1.985(8)	Mo(5)-O(17)	1.665(10)
Mo(5)-O(18)	1.959(9)	Mo(5)-O(19)	1.926(9)
Mo(5)-O(38)	2.434(8)	Mo(6)-O(16)	2.061(8)
Mo(6)-O(18)	1.846(8)	Mo(6)-O(20)	1.671(10)
Mo(6)-O(21)	2.103(8)	Mo(6)-O(22)	1.824(9)
Mo(6)-O(38)	2.383(9)	Mo(7)-O(12)	2.115(9)
Mo(7)-O(23)	1.677(11)	Mo(7)-O(24)	2.061(8)
Mo(7)-O(25)	1.829(9)	Mo(7)-O(26)	1.828(7)
Mo(7)-O(39)	2.394(10)	Mo(8)-O(4)	2.091(9)
Mo(8)-O(19)	1.840(10)	Mo(8)-O(24)	2.062(10)
Mo(8)-O(27)	1.682(7)	Mo(8)-O(28)	1.819(8)
Mo(8)-O(39)	2.394(7)	Mo(9)-O(22)	1.939(10)
Mo(9)-O(25)	1.990(10)	Mo(9)-O(28)	1.986(7)
Mo(9)-O(29)	1.650(9)	Mo(9)-O(30)	1.954(7)
Mo(9)-O(39)	2.434(8)	Mo(10)-O(8)	1.824(8)
Mo(10)-O(15)	2.104(10)	Mo(10)-O(31)	1.692(8)
Mo(10)-O(32)	1.839(10)	Mo(10)-O(33)	2.059(9)
Mo(10)-O(40)	2.383(7)	Mo(11)-O(11)	1.933(8)
Mo(11)-O(26)	1.942(7)	Mo(11)-O(32)	1.972(8)
Mo(11)-O(34)	1.650(11)	Mo(11)-O(35)	1.990(9)
Mo(11)-O(40)	2.424(10)	Mo(12)-O(21)	2.097(10)
Mo(12)-O(30)	1.820(8)	Mo(12)-O(33)	2.078(8)
Mo(12)-O(35)	1.830(10)	Mo(12)-O(36)	1.670(9)
Mo(12)-O(40)	2.382(8)	As(1)-O(4)	1.839(10)
As(1)-O(5)	2.088(9)	As(1)-O(12)	1.824(7)
As(1)-O(24)	2.031(9)	As(2)-O(15)	1.817(9)
As(2)-O(16)	2.050(8)	As(2)-O(21)	1.823(8)
As(2)-O(33)	2.049(10)	As(3)-O(37)	1.683(9)
As(3)-O(38)	1.675(10)	As(3)-O(39)	1.671(8)
As(3)-O(40)	1.691(7)	Na-O(46)	2.282(47)
Na-Mo(1A)	3.686(1)	Na-Mo(1B)	3.686(1)
Na-O(1A)	3.140(8)	Na-O(13A)	2.714(10)
Na-O(13B)	2.714(10)	Na-O(46A)	2.282(47)
O(1)-NaA	3.140(8)		

Table IV. Bond Number Calculations for Selected Atoms in 1

atom	Σs_i, vu	atom	Σs_i, vu
Mo(1)	5.35	Mo(8)	5.38
Mo(2)	5.15	Mo(9)	5.16
Mo(3)	5.40	Mo(10)	5.30
Mo(4)	5.33	Mo(11)	5.20
Mo(5)	5.17	Mo(12)	5.43
Mo(6)	5.44	tot.	63.70
Mo(7)	5.39		

atoms with four Mo_3O_{13} groups, each of which is constructed from three edge-sharing MoO_6 octahedra. These Mo_3O_{13} subunits are in turn joined to each other by corner-sharing to produce the α-Keggin core. The surface of the α-Keggin assembly exhibits four cavities defined by eight-membered $\{Mo_4O_4\}$ rings. The As(III) groups cap two oppositely disposed faces of this type. On the basis of valence sum calculations,[22,23] the bond lengths associated with the As centers, shown in Table III, are consistent with the oxidation state assignments of As(3) as +5 and As(1) and As(2) as +3. The pyramidal geometries of the As(1) and As(2) sites are likewise consistent with As(III) centers with the stereochemically active lone pair occupying the vacant apical site. Curiously, the As(III) sites exhibit rectangular pyramidal $\{AsO_4\}$ geometry, rather than the triangular pyramidal $\{AsO_3\}$ geometry associated with As(III) sites in other polyanions, such as $[H_6As_{10}Mo_{24}O_{90}]^{8-}$ [16] and $[As_8V_{14}O_{42}(0.5H_2O)]^{4-}$.[24]

The presence of the $\{Mo_4O_4\}$ face-capping As(III) groups serves to distort the idealized $\bar{4}3m$ symmetry of the α-Keggin core. The effect is most obvious in the geometry of the four 12-membered $\{Mo_6O_6\}$ rings which girdle the core (Figure 4, supplementary material). The projection of the rings onto a plane reveals that these units are distorted from the idealized regular geometry, so

as to appear flattened at one pole and pointed at the opposite pole. When viewed normal to this planar projection, the origin of the distortion is seen to be related to the out of plane shift of the oxo-groups coordinated to the face-capping As(III) centers. That the distortions are not equivalent at each oxo group of the $\{AsMo_2O\}$ type within the ring is ascribed to the presence of two types of structurally and chemically unique triply bridging oxo groups of the type $\{AsMo_2O\}$. Each of the As(III) sites is coordinated to four oxo groups of a $\{Mo_4O_4\}$ face such that there are two short As–O bond distances of *ca.* 1.82 Å and two longer interactions of 2.05 Å. The triply bridging oxo-groups associated with the longer As–O bonds exhibit pyramidal geometries, while those associated with the shorter As–O distances are more nearly trigonal planar (Figure 5, supplementary material). Valence sum calculations for the latter type are consistent with bond numbers of *ca.* 2.00 for these sites, while those for the former average *ca.* 1.20 valence units. The pyramidal geometries and the valence sum calculations associated with O(5), O(24), O(16), and O(33) thus identify these oxo groups as the protonation sites. Consequently, there are two types of oxygens associated with the capped $\{Mo_4O_4\}$ faces: triply-bridging oxo groups of the $\{AsMo_2O\}$ units and triply-bridging hydroxy groups $\{AsMo_2OH\}$. Returning to the distorted $\{Mo_6O_6\}$ rings, it is noted that each ring contains four doubly-bridging oxo groups, one triply-bridging oxo group, and one triply-bridging hydroxy group. Thus, the two oxygens of each ring which are associated with the As(III) centers are chemically distinct and exhibit significantly different geometric constraints.

The structural analysis of **1a** is consistent with an anion of –1 charge, $[H_4As^{III}_2As^VMo_{12}O_{40}]^-$. The number of protons associated with the core is consistent with the bonding arguments presented above, with the charge of the anion and with titrimetric determinations of the number of Mo(V) centers. The presence of eight Mo(V) centers in **1a** is also confirmed by valence sum calculations based on the bond distances associated with the Mo centers, which are summarized in Table IV. These calculations also indicate that four of the electrons are localized on Mo sites Mo(2), Mo(5), Mo(9), and Mo(11), while the remaining four electrons are effectively delocalized throughout the cluster. Each localized reduced Mo site is associated with a different $\{Mo_3O_{13}\}$ triad; furthermore, the four reduced sites are the Mo centers which do not participate in bonding to triply-bridging oxo or hydroxy groups associated with the As(III) centers.

As shown in Table V, an analysis of the Mo⋯Mo distances of **1a** is consistent with the distortion of the α-Keggin core brought about by the capping of two faces by As(III) groups. The reduced Mo mites, Mo(2), Mo(5), Mo(9), and Mo(11) exhibit Mo⋯Mo distances which are marginally shorter than those observed for α-$[PW_{12}O_{40}]^{3-}$ [25] and α-$[PMo_{12}O_{40}]^{3-}$ [26] and shorter than those for the remaining Mo⋯Mo interactions of **1a**. The net effect of face capping of the α-Keggin core by the As(III) groups is the not unanticipated expansion of the majority of the Mo⋯Mo distances which are associated with the eight Mo centers involved

(22) Brown, I. D.; Shannon, R. D. *Acta Crystallogr., Sect. A* **1973**, *29*, 266.
(23) Brown, I. D.; Wu, K. K. *Acta Crystallogr., Sect. B* **1976**, *32*, 1976.
(24) Huan, G.; Greaney, M. A.; Jacobson, A. J. *J. Chem. Soc., Chem. Commun.* **1991**, 260.

(25) Brown, G. M.; Noe-Spirlet, M. R.; Busing, W. R.; Levy, H. A. *Acta Crystallogr., Sect. B* **1977**, *B33*, 1038.
(26) D'Amour, H.; Allmann, R. *Z. Kristallogr.*, Kristallgeom., Kristallphys., Kristallchem. **1976**, *143*, 1.
(27) Feist, M.; Molchanov, V. N.; Kazanskii, L. P.; Torchenkova, E. A.; Spitsyn, V. I. *Russ. J. Inorg. Chem. (Engl. Trans.)* **1980**, *5*, 401.

Table V. Mo···Mo Distances

(a) Mo···Mo Distances in **1**

Mo(1)–Mo(2)	3.382	Mo(6)–Mo(9)	3.696
Mo(2)–Mo(3)	3.547	Mo(6)–Mo(12)	3.980
Mo(1)–Mo(5)	3.708	Mo(7)–Mo(8)	3.558
Mo(1)–Mo(8)	3.977	Mo(7)–Mo(9)	3.390
Mo(2)–Mo(3)	3.393	Mo(7)–Mo(11)	3.702
Mo(2)–Mo(4)	3.705	Mo(8)–Mo(9)	3.384
Mo(2)–Mo(10)	3.699	Mo(9)–Mo(12)	3.698
Mo(3)–Mo(7)	3.977	Mo(10)–Mo(11)	3.379
Mo(3)–Mo(11)	3.700	Mo(10)–Mo(12)	3.559
Mo(4)–Mo(5)	3.393	Mo(11)–Mo(12)	3.399
Mo(4)–Mo(6)	3.534		
Mo(4)–Mo(10)	3.989		
Mo(5)–Mo(6)	3.375		
Mo(5)–Mo(8)	3.697		

(b) A Comparison of Average Mo···Mo Distances in
1 to Those in Other Keggin Structures

Anion	distances		ref
	Mo–Mo (edge-linked)	Mo–Mo (corner-linked)	
α-[PW$_{12}$O$_{40}$]$^{3-}$	3.41	3.70	25
α-[PMo$_{12}$O$_{40}$]$^{3-}$	3.41	3.71	26
α-[SiMo$_{12}$O$_{40}$]$^{4-}$	3.36	3.70	27
β-[H$_6$PMo$_{12}$O$_{40}$]$^{1-}$	3.41–3.56	3.65–3.77	4
β-[H$_4$AsMo$_{12}$O$_{40}$]$^{3-}$	3.41–3.61	3.64–3.71	16
α-[H$_4$As$_3$Mo$_{12}$O$_{40}$]$^{1-}$	3.38–3.56	3.70–3.99	this work

in bonding to oxygen atoms bridging to these As(III) sites. The Mo···Mo separations most significantly lengthened are those between Mo pairs bridged by the triply-bridging, approximately trigonal planar oxo groups. Comparison of the Mo···Mo distances of **1a** to those for the two other examples of reduced Mo–Keggin species also suggests that the predominant structural determinant is the face-capping of the As(III) rather than the reduction and protonation of the core. It should be noted that the previously described reduced Mo–Keggin species possess the β-Keggin structure, i.e., one in which one of the {Mo$_3$O$_{13}$} triads is rotated by 60° to give a figure of idealized C_3 symmetry. Cluster **1a** is a unique example of a structurally characterized reduced α-Keggin core.

The Na$^+$ cation is located on a crystallographic center of symmetry, apparently with a measure of disorder about the site, and displays distorted octahedral geometry through coordination to two aquo ligands and two terminal oxo groups and two doubly-bridging oxo groups of four symmetry-related clusters. These cation/cluster units connect to generate linear strips two anion units in thickness parallel to the crystallographic *a* axis, (Figure 6, supplementary material). When viewed down the *a* axis, these strips appear as parallel anion stacks bridged by [Na(H$_2$O)$_2$]$^+$ groups. The water molecules of crystallization occupy the large polar cavities which are generated between the anion stacks. The size of the cavity and the extensive disorder associated with the waters of crystallization are consistent with the facile removal of the water in the TGA and with the loss of crystallinity consequent to removal of **1** from the mother liquor at room temperature.

Conclusions

Hydrothermal synthesis has been exploited to prepare a novel α-Keggin based cluster, [H$_4$As$^{III}_2$As^{V}Mo$^V_8$Mo$^{VI}_4$O$_{40}$]$^-$ (**1a**). Cluster **1a** is an example of a derivatized α-Keggin core, bicapped on opposite {Mo$_4$O$_4$} faces by As(III) groups. As such it is a unique example of an As(III)/As(V) polyoxometalate cluster. Compound **1a** is also a relatively unusual example of a crystalline mixed-valence Mo–Keggin structure. The cluster is highly reduced with eight Mo centers formally in the +5 oxidation state. Highly reduced polymetalate structures are an emerging theme of the hydrothermal chemistry of Mo and V in the presence of ligands capable of capping faces of the parent cores.